Received June 2004
Reviewed February 2005
Accepted April 2005

Solid velocity correction schemes for a temperature transforming model for convection phase change

Zhanhua Ma
Department of Mechanical and Aerospace Engineering, Princeton University, Princeton, New Jersey, USA, and
Yuwen Zhang
Department of Mechanical and Aerospace Engineering, University of Missouri-Columbia, Columbia, Missouri, USA

Abstract

Purpose – To study the effects of velocity correction schemes for a temperature transforming model (TTM) for convection controlled solid-liquid phase-change problem.

Design/methodology/approach – The effects of three different solid velocity correction schemes, the ramped switch-off method (RSOM), the ramped source term method (RSTM) and the variable viscosity method (VVM), on a TTM for numerical simulation of convection controlled solid-liquid phase-change problems are investigated in this paper. The comparison is accomplished by analyzing numerical simulation and experimental results of a convection/diffusion phase-change problem in a rectangular cavity. Model consistency of the discretized TTM is also examined in this paper. The simulation results using RSOM, RSTM and VVM in TTM are compared with experimental results.

Findings – In order to efficiently use the discretized TTM model and obtain convergent and reasonable results, a grid size must be chosen with a suitable time step (which should not be too small). Applications of RSOM and RSTM-TTM yield identical results which are more accurate than VVM.

Originality/value – This paper provides generalized guidelines about the solid velocity correction scheme and criteria for selection of time step/grid size for the convection controlled phase change problem.

Keywords Convection, Heat transfer, Melting, Numerical analysis

Paper type Research paper

Nomenclature

a	= coefficient in equation (16)
b	= term in equation (16)
c	= specific heat (J/(kg K))
c^0	= coefficient in equation (4) (J/(kg K))
C	= c^0/c_l
C_{sl}	= c_s/c_l
d	= coefficient in velocity correction equations (17) and (18)
g	= gravitational acceleration, 9.8 m/s^2
H	= height of the vertical wall (m)
k	= thermal conductivity (W/(m K))
K	= dimensionless thermal conductivity, k/k_l
K_{sl}	= k_s/k_l
L	= latent heat (J/kg)
p	= pressure (N/m^2)
P	= dimensionless pressure, $(p + \rho_\infty g y)H^2/\rho\nu_l^2$.
P^*	= initially guessed dimensionless pressure
P'	= pressure correction
Pr	= Prandtl number, ν/α_l.

International Journal of Numerical Methods for Heat & Fluid Flow
Vol. 16 No. 2, 2006
pp. 204-225

0961-5539
DOI 10.1108/09615530610644271

Pr_{l} = Prandtl number of liquid, $\nu_{\mathrm{l}}/\alpha_{\mathrm{l}}$.
Pr_{m} = Prandtl number of mushy phase, $Pr_{\mathrm{l}} + (Pr_{\mathrm{l}} - Pr_{\mathrm{s}}) \times (T - \delta T^{*})/(2\delta T^{*})$.
Ra = Raleigh number, $g\beta \mathrm{H}^3 (T_h^0 - T_c^0)/\nu_{\mathrm{l}}\alpha_{\mathrm{l}}$.
S^0 = term in B
S = $S^0/c_{\mathrm{l}}(T_h^0 - T_c^0)$.
S_c = linearized source term in equation (19)
S_p = linearized source term in equation (19)
Ste = Stefan number, $c_{\mathrm{l}}(T_h^0 - T_c^0)/L$.
T = dimensionless temperature, $(T^0 - T_m^0)/(T_h^0 - T_c^0)$.
T_i = dimensionless initial temperature
T^0 = temperature, K
T^* = scaled temperature, $T^0 - T_m^0$, K
T_c^0 = cold surface temperature, K
T_m^0 = melting (or freezing) temperature, K
T_h^0 = hot surface temperature, K
T = time, s
u, v = velocities, m/s
U, V = dimensionless velocities, uH/ν_{l}, $v\mathrm{H}/\nu_{\mathrm{l}}$.
U^*, V^* = dimensionless velocities computed from P^*
X, Y = dimensionless coordinate directions, x/H, y/H.
x, y = coordinate, m

Greek symbols
α = thermal diffusivity (m²/s)
β = coefficient of volumetric thermal expansion, 1/K
$2\delta T^0$ = phase-change temperature range, $T_l^0 - T_s^0$.
δT^* = $\delta T^0/(T_h^0 - T_c^0)$.
ε_{l} = the ratio of the volume of liquid to the total volume of the computational domain
ϕ = general dependent variable, equation (16)
ρ = density (kg/m³), $\rho = \rho_\infty(1 - \beta(T^0 - T_m^0))$.
ρ_∞ = reference density (kg/m³)
μ = dynamic viscosity (kg/(m − s))
ν = kinematic viscosity (m²/s)
τ = dimensionless time, $\nu_{\mathrm{l}}t/\mathrm{H}^2$.

Subscripts
E = east neighbor of grid P
e = control-volume face between P and E
i = initial value
l = liquid phase
m = mushy phase
n = control-volume face between P and N
N = north neighbor of grid P
nb = neighbors of grid P
P = grid point
s = solid phase or control-volume face between P and S
S = south neighbor of grid P
w = control-volume face between P and W
W = west neighbor of grid P

1. Introduction

Modeling and numerical simulation for solid-liquid phase-change problems has become an active area in the last several decades (Viskanta, 1983; Yao and Prusa, 1989). Research in this area is motivated by new technology applications in energy systems (Zhang and Faghri, 1996) as well as manufacturing, such as laser drilling (Zhang and Faghri, 1999), laser welding (Mundra *et al.*, 1996), and selective laser sintering (Zhang *et al.*, 2000). To develop an accurate and stable numerical simulation method of the dynamic process of a solid-liquid phase change, we are above all facing the following two challenges:

(1) Development of a reliable model for convection-controlled heat transfer problems, which is important because the heat convection caused by fluid flow usually dominates the heat transfer process in a liquid region in those solid phase-change problems.

(2) How to make that model suitable for phase-change problems including moving melting/solidification fronts in the computed domain.

In the last-20 years a large number of numerical techniques have been developed, which can be broadly divided into two groups (Voller, 1997): fixed grid schemes (or weak numerical solutions) and deforming grid schemes (or strong numerical solutions). Fixed grid schemes have a much simpler mathematical structure than deforming grid scheme yet are reasonably accurate and fast (Morgan, 1981; Voller *et al.*, 1987; Cao and Faghri, 1990; Sasaguchi *et al.*, 1996; Voller, 1997; Binet and Lacroix, 2000). There are two widely used methods in the group of fixed grid schemes: enthalpy method (Voller *et al.*, 1987; Binet and Lacroix, 2000), and temperature-based equivalent heat capacity methods (Morgan, 1981; Hsiao, 1984). The enthalpy method can deal with both mushy and isothermal phase-change problems but the temperature at a typical grid point may oscillate with time. The temperature-based method, on the other hand, generates results without oscillations but has difficulty handling cases where the phase-change temperature range is small. To overcome these drawbacks, Cao and Faghri (1990) proposed an improved temperature-based equivalent heat capacity method, the temperature transforming model (TTM), in which the enthalpy-based energy equation is converted into a nonlinear equation with a single dependent variable. The simulation results of the TTM method shown by Cao and Faghri (1990) are accurate enough compared with experimental results and it also features a simple structure and an efficient simulation time. For these reasons the present authors chose the TTM method for simulations on convection/diffusion phase-change problems.

Before applying this TTM method for phase-change problems we must determine how to express the solid and liquid phases in the model. In a solid region the velocity of phase change materials (PCM) should be set to zero. In a liquid region the velocity must be solved from the corresponding momentum and continuity equations. Currently, there are three widely used families of solid velocity correction schemes for this purpose: they are the switch-off method (SOM) (Voller *et al.*, 1987; Yang and Tao, 1992), the variable viscosity method (VVM) (Gartling, 1980; Voller *et al.*, 1987; Cao and Faghri, 1990), and the source term method (STM) (Voller *et al.*, 1987; Brent *et al.*, 1988; Voller, 1997; Yang and Tao, 1992; Sasaguchi *et al.*, 1996; Binet and Lacroix, 2000). Note that in Voller *et al.* (1987) and Brent *et al.*'s (1988) work, a special kind of STM, Darcy STM, was developed in the context of enthalpy method. This Darcy STM is essentially similar to the ramped source term method (RSTM) method for TTM, on which we will discuss in detail in the following sections. Voller *et al.* (1987) compared the Darcy STM, VVM and SOM and concluded that the Darcy source-term method is more stable than the other two.

Since Voller *et al.*'s (1987) comparison was based on a model using only enthalpy-method, and the Darcy STM in TTM is not applicable, it is necessary to validate and compare SOM, STM and VVM on a TTM model as it used in convection/diffusion phase-change problems. The objectives of this paper are to validate two modified schemes, the ramped switch-off method (RSOM) and the RSTM, and compare them with VVM. The comparative results (in convergence, accuracy and simulation speed) by running a series of numerical simulation tests for a two-dimensional example will be presented recommendations on how to choose an appropriate combinations of grid sizes and time step for numerical simulation of convection/diffusion phase-change problems will also be made.

2. Temperature transforming model for convection controlled solid-liquid phase-change problems

The TTM was proposed by Cao and Faghri (1990) for solving typical PCM phase-change problems including the effect of natural convection. This model is based on the following assumptions:

- the PCM is pure, homogeneous and with a mushy phase change;
- the liquid phase of the PCM is considered a Newtonian, incompressible fluid;
- radiation effects and viscous dissipation are neglected; and
- the change of the values of these thermophysical properties in the mushy region is linear.

In TTM, general continuity and momentum equations for fluid problems are used, while its energy equation is different from the enthalpy-based energy equations applied in traditional temperature-based equivalent heat capacity methods. The governing equations of TTM expressed in a two-dimensional Cartesian coordinate system are as follows (y-axis is the vertical axis).

Continuity equation:

$$\frac{\partial u}{\partial x}+\frac{\partial v}{\partial y}=0 \tag{1}$$

Momentum equations in x and y directions, respectively:

$$\frac{\partial(\rho u)}{\partial t}+\frac{\partial(\rho u^2)}{\partial x}+\frac{\partial(\rho uv)}{\partial y}=-\frac{\partial p}{\partial x}+\rho g_x+\frac{\partial}{\partial x}\left(\mu\frac{\partial u}{\partial x}\right)+\frac{\partial}{\partial y}\left(\mu\frac{\partial u}{\partial y}\right) \tag{2}$$

$$\frac{\partial(\rho v)}{\partial t}+\frac{\partial(\rho uv)}{\partial x}+\frac{\partial(\rho v^2)}{\partial y}=-\frac{\partial p}{\partial y}+\rho g_y+\frac{\partial}{\partial x}\left(\mu\frac{\partial v}{\partial x}\right)+\frac{\partial}{\partial y}\left(\mu\frac{\partial v}{\partial y}\right) \tag{3}$$

Energy equation (Cao and Faghri, 1990):

$$\frac{\partial(\rho c^0T^*)}{\partial t}+\frac{\partial(\rho uc^0T^*)}{\partial x}+\frac{\partial(\rho vc^0T^*)}{\partial y}=\frac{\partial}{\partial x}\left(k\frac{\partial T^*}{\partial x}\right)+\frac{\partial}{\partial y}\left(k\frac{\partial T^*}{\partial y}\right)-\left[\frac{\partial(\rho S^0)}{\partial t}+\frac{\partial(\rho uS^0)}{\partial x}+\frac{\partial(\rho vS^0)}{\partial y}\right] \tag{4}$$

where $T^*=T^0-T_m^0$ is scaled temperature. The coefficients c^0 and S^0 in equation (4) are:

$$c^0(T^*) = \begin{cases} c_s & (T^* < -\delta T^0) \\ \dfrac{c_l + c_s}{2} + \dfrac{L}{2\delta T^0} & (-\delta T^0 \leq T^* \leq \delta T^0) \\ c_l & (T^* > \delta T^0) \end{cases} \tag{5}$$

$$S^0(T^*) = \begin{cases} c_s \delta T^0 & (T^* < -\delta T^0) \\ \dfrac{c_l + c_s}{2} \delta T^0 + \dfrac{L}{2} & (-\delta T^0 \leq T^* \leq \delta T^0) \\ c_s \delta T^0 + L & (T^* > \delta T^0) \end{cases} \tag{6}$$

and the thermal conductivity is:

$$k(T^*) = \begin{cases} k_s & (T^* < -\delta T^0) \\ k_s + (k_l - k_s) \dfrac{T^* + \delta T^0}{2\delta T^0} & (-\delta T^0 \leq T^* \leq \delta T^0) \\ k_l & (T^* > \delta T^0) \end{cases} \tag{7}$$

where $T^* < -\delta T^0$ corresponds to the solid phase, $-\delta T^0 \leq T^* \leq \delta T^0$ to the mushy region, and $T^* > \delta T^0$ to the liquid phase.

Introducing these following non-dimensional variables:

$$X = \frac{x}{H}, \quad Y = \frac{y}{H}, \quad U = u\frac{H}{\nu_l}, \quad V = v\frac{H}{\nu_l}, \quad \tau = \frac{\nu_l t}{H^2}, T = \frac{T^0 - T_m^0}{T_h^0 - T_c^0},$$

$$\delta T^* = \frac{\delta T^0}{T_h^0 - T_c^0}, \quad C = \frac{c^0}{c_l}, \quad S = \frac{S^0}{c_l(T_h^0 - T_c^0)}, \tag{8}$$

$$K = \frac{k}{k_l}, Ste = \frac{c_l\left(T_h^0 - T_c^0\right)}{L}, \quad C_{sl} = \frac{c_s}{c_l}, \quad K_{sl} = \frac{k_s}{k_l}, \quad P = \frac{H^2}{\rho \nu_l^2}(p + \rho_\infty g y)$$

Equations (1)-(7) can be non-dimensionalized as:

$$\frac{\partial U}{\partial X} + \frac{\partial V}{\partial Y} = 0 \tag{9}$$

$$\frac{\partial U}{\partial \tau} + \frac{\partial (U^2)}{\partial X} + \frac{\partial (UV)}{\partial Y} = -\frac{\partial P}{\partial X} + \frac{\partial}{\partial X}\left(\frac{Pr}{Pr_l}\frac{\partial U}{\partial X}\right) + \frac{\partial}{\partial Y}\left(\frac{Pr}{Pr_l}\frac{\partial U}{\partial Y}\right) \tag{10}$$

$$\frac{\partial V}{\partial \tau} + \frac{\partial (UV)}{\partial X} + \frac{\partial (V^2)}{\partial Y} = -\frac{\partial P}{\partial Y} + \frac{Ra}{Pr_l}T + \frac{\partial}{\partial X}\left(\frac{Pr}{Pr_l}\frac{\partial V}{\partial X}\right) + \frac{\partial}{\partial Y}\left(\frac{Pr}{Pr_l}\frac{\partial V}{\partial Y}\right) \tag{11}$$

$$\frac{\partial(CT)}{\partial\tau}+\frac{\partial(UCT)}{\partial X}+\frac{\partial(VCT)}{\partial Y}=\frac{\partial}{\partial X}\left(\frac{K}{Pr_1}\frac{\partial T}{\partial X}\right)+\frac{\partial}{\partial Y}\left(\frac{K}{Pr_1}\frac{\partial T}{\partial Y}\right)$$
$$-\left[\frac{\partial S}{\partial\tau}+\frac{\partial(US)}{\partial X}+\frac{\partial(VS)}{\partial Y}\right] \tag{12}$$

where

$$C(T)=\begin{cases} C_{\mathrm{sl}} & (T<-\delta T^*)\\ \frac{1}{2}(1+C_{\mathrm{sl}})+\frac{1}{2Ste\cdot\delta T^*} & (-\delta T^*\leq T\leq\delta T^*)\\ 1 & (T>\delta T^*)\end{cases} \tag{13}$$

$$S(T)=\begin{cases} C_{\mathrm{sl}}\delta T^* & (T<-\delta T^*)\\ \frac{1}{2}(1+C_{\mathrm{sl}})\delta T^*+\frac{1}{2Ste} & (-\delta T^*\leq T\leq\delta T^*)\\ C_{\mathrm{sl}}\delta T^*+\frac{1}{Ste} & (T>\delta T^*)\end{cases} \tag{14}$$

and

$$K(T)=\begin{cases} K_{\mathrm{sl}} & (T<-\delta T^*)\\ K_{\mathrm{sl}}+(1-K_{\mathrm{sl}})\frac{T+\delta T^*}{2\delta T^*} & (-\delta T^*\leq T\leq\delta T)\\ 1 & (T>\delta T^*)\end{cases} \tag{15}$$

3. Numerical solution procedure

3.1 Discretization of governing equations

The two-dimensional governing equations are discretized by applying a finite volume method (Pantankar, 1980), in which conservation laws are applied over finite-sized control volumes around grid points and the governing equations are then integrated over the volume. Staggered grid arrangement (Pantankar, 1980) is used in the discretization of the computational domain in momentum equations. A power law scheme (Pantankar, 1980) is used to discretize convection/diffusion terms in momentum and energy equations. The main algebraic equation resulting from this control volume approach is in the form of:

$$a_{\mathrm{P}}\phi_{\mathrm{P}}=\sum a_{\mathrm{nb}}\phi_{\mathrm{nb}}+b \tag{16}$$

where ϕ_{P} represents the value of variable ϕ (U, V or T) at the grid point P, ϕ_{nb} are the values of the variable at P's neighbor grid points, and a_{P}, a_{nb} and b are corresponding coefficients and terms derived from original governing equations. The numerical simulation is accomplished by using Simple algorithm (Pantankar, 1980). Note that the velocity-correction equations for corrected U and V in the algorithm are:

$$U_e = U_e^* + d_e(P'_P - P'_E) \quad (17)$$

$$V_n = V_n^* + d_n(P'_P - P'_N) \quad (18)$$

where according to the staggered grid arrangement e and n, respectively, represent the control-volume faces between grid P and its east neighbor E and grid P and its north neighbor N. The source term S in governing equations is linearized in the form

$$S = S_C + S_P \phi_P \quad (19)$$

in a control volume, and by discretization S_P and S_C are then, respectively, included in a_P and b in equation (16).

3.2 Three alternative solid velocity correction schemes for phase-change problems
Having chosen the TTM model and Simple algorithm for numerical simulations, we now turn our attention to developing a reliable solid velocity correction scheme to ensure that velocities in the solid region will be kept equal to zero during simulations of phase-change problems. In this subsection, three commonly used families of solid velocity correction schemes for phase-change problems, i.e. SOM, STM and VVM, as well as two modified versions of SOM and STM, i.e. RSOM and RSTM, will be discussed.

3.3 Switch-off method (SOM)/ramped switch-off method (RSOM)
The SOM is the most straightforward method (Morgan, 1981; Voller *et al.*, 1987; Yang and Tao, 1992). It divides the whole domain into a solid region (where $T < 0$) and a liquid region (where $T \geq 0$), and then directly sets the velocities U and V in the solid area to be zero by setting the coefficients a_P in discretized U and V momentum equations (in form of equation (16) where ϕ represents U or V) equal to a very large positive number and the coefficients d_e and d_n in the U and V velocity-correction equations, equations (17) and (18), equal to very small positive numbers (Yang and Tao, 1992). For instance, in Yang and Tao (1992), $a_P = 10^{30}$ and $d_e = d_n = 10^{-30}$. The small values of d_e and d_n guarantee that the values of U and V stay very small during the process of solving the velocity-correction equations (17) and (18). The values of a_P, d_e and d_n in the liquid region (where $T \geq 0$) are directly calculated from Simple algorithm.

Although this (conventional) SOM method is commonly used in numerical simulations of phase-change problems, our simulations show that if used together with a TTM model for convection controlled solid-liquid phase-change problems, the SOM will result in a serious inconsistency of the TTM model (see Section 4, point 3 for detailed discussion about the inconsistency) and consequently cannot provide accurate simulation results. In the example, a solid-liquid phase change with convection/diffusion in a vertically positioned two-dimensional cavity case is considered (Figure 1; Okada, 1984). TTM and Simple algorithm are applied for numerical simulations. The boundary and initial conditions are $T_i = 0$, and $T_c = 0$ and $T_h = 1$ for $\tau \geq 0$. The upper and lower boundaries of the cavity are insulated. To conduct numerical simulations, the half dimensionless phase-change temperature is set as $\delta T^* = 0.01$ and the initial conditions the temperature $T(x, y; t)$ are set as: $T(x, y; 0) = T_i = -0.01$. The boundary conditions are $T(0, y; t) = T_h = 1$, $T(1, y; t) = T_c = -0.01$, and adiabatic conditions are applied at bottom and top of the domain. Other parameters are set as follows: $Ra = 3.27 \times 10^5$, $Pr_1 = 56.2$,

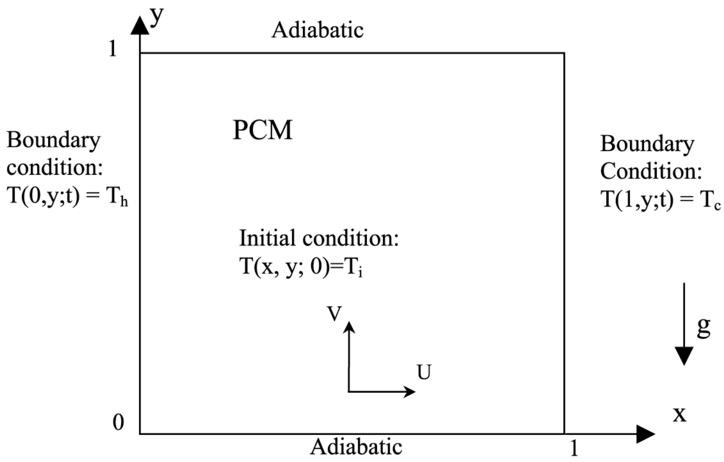

Figure 1. Melting in a vertical two-dimensional cavity

$Ste = 0.045$, $C_{sl} = 1.0$ and $K_{sl} = 1.0$. During simulations the values of the underrelaxation factors for U, V, T and P are, respectively, taken as 0.1, 0.1, 0.1 and 0.12.

The simulation results using SOM obtained by running the simulation to a dimensionless time of $\tau = 100$ are listed in Tables I-III, where ε_l represents the ratio of the volume of liquid to the total volume of the cavity. These results show that when time step is smaller than ten, SOM will diverge and thus accurate simulation results

$\Delta\tau$ (dimensionless time step)		20	10	5	1	0.5	0.1	0.01
SOM	Convergence	Yes	Yes	No	No	No	No	No
	ε_l (percent)	53.266	60.603	–	–	–	–	–
STM	Convergence	Yes	Yes	No	No	No	No	No
	ε_l (percent)	53.265	60.604	–	–	–	–	–

Table I. Simulation results with a grid size of 20×20 (stopped when $\tau = 100$)

$\Delta\tau$ (dimensionless time step)		20	10	5	1	0.5	0.1	0.01
SOM	Convergence	Yes	Yes	No	No	No	No	No
	ε_l (percent)	52.284	58.038	–	–	–	–	–
STM	Convergence	Yes	Yes	No	No	No	No	No
	ε_l (percent)	52.285	58.038	–	–	–	–	–

Table II. Simulation results with a grid size of 40×40 (stopped when $\tau = 100$)

$\Delta\tau$ (dimensionless time step)		20	10	5	1	0.5	0.1	0.01
SOM	Convergence	Yes	Yes	No	No	No	No	No
	ε_l (percent)	49.778	55.122	–	–	–	–	–
STM	Convergence	Yes	Yes	No	No	No	No	No
	ε_l (percent)	49.775	55.121	–	–	–	–	–

Table III. Simulation results with a grid size of 80×80 (stopped when $\tau = 100$)

cannot be obtained. This is because TTM uses a mushy region to guarantee that the temperature T is continuous in the whole computed domain, while in SOM, the values of velocity variables U and V are discontinuous at the solid-liquid phase-change fronts, which causes deterioration of the model and result in inconsistency. SOM must, therefore, be modified before they can be implemented in TTM. Naturally, with the mushy region assumption in TTM, a ramped SOM, RSOM, is worth trying to avoid the discontinuity.

In RSOM, the whole domain is divided into three regions: solid region, mushy region and liquid region. The values of a_{P}, d_e and d_n in the solid area ($T \leq -\delta T^*$) are set as very large positive numbers (here choose $a_{\mathrm{P}} = 10^{30}$, $d_e = d_n = 10^{-30}$), while in the mushy region where $-\delta T^* \leq T \leq \delta T^*$, the adjustments for a_{P}, d_e and d_n satisfy the following linear relations:

$$a_{\mathrm{P}} = a_{Pi} + (a_{Pi} - 10^{30})\frac{T - \delta T^*}{2\delta T^*}$$

$$d_e = \frac{d_{ei}}{a_{\mathrm{P}}}, \quad d_n = \frac{d_{ni}}{a_{\mathrm{P}}}$$

where a_{Pi}, d_{ei} and d_{ni} are the values of these coefficients in the mushy region originally computed by Simple algorithm. For the liquid area ($T \geq \delta T^*$), a_{P}, d_e and d_n are just directly computed by the Simple algorithm.

Now that all values of variables U and V and their relative coefficients become continuous in the whole computational domain in the RSOM, this scheme is expected to perform better than SOM in numerical simulations based on the TTM model (See Section 4 for simulation results and discussions).

3.4 Source term method (STM)/ramped source term method (RSTM)

The STM (Yang and Tao, 1992) is essentially also a kind of "switch-off" method. This method normally sets the velocities U and V of an internal grid point in the solid region (where $T < 0$) equal to zero by imposing the corresponding linearized source terms S_C equal to a very large positive number times the desired values of U or V (which are zero here) and S_{P} equal to a very large negative number. For instance, in Yang and Tao (1992), $S_c = 10^{30}\phi_{\mathrm{P}} = 0$ and $S_C = -10^{30}$, where ϕ represents U or V. The values of S_C and S_{P} in liquid regions (where $T \geq 0$) are directly calculated from Simple algorithm.

Same as SOM, this STM also suffers from discontinuity at the front of phase change and, therefore, is not suitable for simulations on phase-change problems based on TTM (see Tables I-III as examples). Thus, similar to RSOM, a RSTM, should be introduced. As mentioned before, in Voller *et al.* (1987) and Brent *et al.* (1988), a Darcy STM (with linear or nonlinear settings) was developed for phase-change simulations in the context of enthalpy method. It is indeed a kind of RSTM since it ramps the value of the switch based on Darcy's law. In our TTM model, the setting of (linear) RSTM is as following.

In the solid area ($T \leq -\delta T^*$), coefficients of source terms in momentum equations are set as $S_C = 0$ and $S_{\mathrm{P}} = -10^{30}$. In the mushy region ($-\delta T^* \leq T \leq \delta T^*$):

$$S_{\mathrm{P}} = S_{Pi} + (S_{Pi} + 10^{30})\frac{T - \delta T^*}{2\delta T^*}$$

$$S_C = S_{Ci} + (S_{Ci} - 0)\frac{T - \delta T^*}{2\delta T^*}$$

where S_{pi} and S_{ci} are the values of S_p and S_c originally computed by Simple method, and in the liquid area ($T \geq \delta T^*$), Simple method generates the corresponding S_p and S_c.

3.5 Variable viscosity method (VVM)

The VVM was proposed by Gartling (1980) and also used in, for example, Cao and Faghri (1990). It divides the computational domain into solid area, mushy region and liquid region. The governing equations (9)-(12) are valid in the whole domain, and the velocities U and V are computed by solving these equations with different Prandtl numbers (which represent viscosity) in different regions. In our model, the Prandtl number is set as $Pr_s = 56.2 \times 10^{30}$ in the solid region ($T \leq -\delta T^*$), $Pr_l = 56.2$ in the liquid region ($T \geq \delta T^*$), and $Pr_m = Pr_l + (Pr_l - Pr_s)(T - \delta T^*)/(2\delta T^*)$ in the mushy region ($-\delta T^* \leq T \leq \delta T^*$). The large Prandtl number in the solid area guarantees zero velocities.

In the next section we will use the example from Okada (1984) to compare the RSOM, RSTM and VVM to each other and experimental results to evaluate their effects on the TTM model used in convection controlled solid-liquid phase-change problems.

4. Results and discussions

Okada's (1984) case (Figure 1) is used here for comparison of effects of RSOM, RSTM and VVM on a TTM model in convection controlled solid-liquid phase-change problems. Tables IV-VI list the simulation results obtained by running the simulation program until a dimensionless time $\tau = 100$. Figures 2-4 show the positions of melting fronts obtained by RSOM, RSTM and VVM compared with comparison with Okada's (1984) experimental results and Cao and Faghri's (1990) simulation results when $\tau = 39.9$. Figures 5-7 show those positions at $\tau = 78.68$. Note that in the tables "convergence" only means that the simulation does not blow up to infinity during the iterations. Strictly speaking, those results denoted by "*" are also divergent since they do not converge to the correct values.

From these results we can see the following.

Comparison between RSOM and RSTM. The numerical results obtained by using RSOM and RSTM, including the convergence property, ε_l, the positions of the melting fronts during the simulation and number of iterations (the convergence speed), are almost the same. Therefore, RSOM and RSTM can be regarded as equivalent for this problem simulated by TTM. Since the essences of both RSOM and RSTM is to set certain coefficients in the algebraic equations derived from the control volume approach (i.e. $a_P \phi_P = \sum a_{nb}\phi_{nb} + b$) equal to very large numbers and then resulting in the corresponding ϕ_P (here is U or V) being almost zero, it is not surprising that these two schemes generated almost identical results.

Recall that in Voller *et al.* (1987), the conclusion was that the Darcy STM performs better than a non-ramped SOM for simulations using enthalpy method. It is easy to explain since a continuous RSTM is better than a discontinuous SOM. To develop a RSOM scheme for enthalpy method and then compare it with Darcy STM will be interesting.

Table IV.
Simulation results with a grid size of 20×20 (stopped when $\tau = 100$)

$\Delta\tau$ (dimensionless time step)		20	10	5	1	0.5	0.1	0.05	0.01	0.005	0.001
$\Delta\tau/\Delta X\Delta Y$		8000	4000	2000	400	200	40	20	4	2	0.4
RSOM	Convergence	Yes	Yes	Yes	Yes	Yes	No	Yes	Yes	Yes	Yes
	ε_1 (percent)	50.755	55.285	59.703	63.558	64.135	–	55.043	19.026[a]	16.513[a]	13.092[a]
	Number of iterations	9,720	16,361	26,959	66,131	90,384	–	120,500	44,319	56,254	120,865
RSTM	Convergence	Yes	Yes	Yes	Yes	Yes	No	Yes	Yes	Yes	Yes
	ε_1 (percent)	50.755	55.285	59.703	63.558	64.135	–	54.934	19.025[a]	16.513[a]	13.092[a]
	Number of iterations	9,399	16,598	26,947	66,098	90,336	–	119,961	44,283	56,281	12,0868
VVM	Convergence	Yes	Yes	Yes	Yes	Yes	No	Yes	Yes	No	No
	ε_1 (percent)	49.842	53.879	58.040	61.609	62.099	–	53.455	17.903[a]	–	–
	Number of iterations	9,484	16,190	25,706	63,848	84,307	–	112,695	38,187	–	–

Note: [a]Convergent to unreasonable results

Table V. Simulation results with a grid size of 40×40 (stopped when $\tau = 100$)

$\Delta\tau$ (dimensionless time step)		20	10	5	1	0.5	0.1	0.05	0.01	0.005	0.001
$\Delta\tau/\Delta X\Delta Y$		32000	16000	8000	1600	800	160	80	16	8	1.6
RSOM	Convergence	Yes	Yes	Yes	Yes	Yes	Yes	No	Yes	Yes	Yes
	ε_1 (percent)	49.387	54.545	59.126	63.901	64.653	65.118	–	42.371	29.638[a]	16.474[a]
	Number of iterations	12,320	21,651	33,805	85,288	118,896	216,729	–	283,438	239,313	247,966
RSTM	Convergence	Yes	Yes	Yes	Yes	Yes	Yes	No	Yes	Yes	Yes
	ε_1 (percent)	49.405	54.545	59.125	63.901	64.653	65.119	–	42.393	29.641[a]	16.473[a]
	Number of iterations	12,334	21,656	33,809	85,244	119,437	216,721	–	283,654	239,264	247,953
VVM	Convergence	Yes	Yes	Yes	Yes	Yes	Yes	Yes	No	No	No
	ε_1 (percent)	48.481	53.292	57.502	61.962	62.691	63.144	62.660	–	–	–
	Number of iterations	12,126	21,248	33,340	82,521	113,949	211,264	266476	–	–	–

Note: [a]Convergent to unreasonable results

Table VI. Simulation results with a grid size of 80 × 80 (stopped when $\tau = 100$)

$\Delta\tau$ (dimensionless time step)		20	10	5	1	0.5	0.1	0.05	0.01	0.005	0.001
$\Delta\tau/\Delta X\Delta Y$		128000	64000	32000	6400	3200	640	320	64	32	6.4
RSOM	Convergence	Yes	Yes	Yes	Yes	Yes	Yes	Yes	Yes	Yes	Yes
	ε_1 (percent)	47.939	52.771	56.910	62.232	62.996	63.787	63.927	62.097	53.741	23.779[a]
	Number of iterations	28,580	43,751	69,884	144,207	185,937	387,260	514,673	815,871	853,218	606,342
RSTM	Convergence	Yes	Yes	Yes	Yes	Yes	Yes	Yes	Yes	Yes	Yes
	ε_1 (percent)	47.939	52.771	56.910	62.232	62.996	63.787	63.927	62.044	53.746	23.779[a]
	Number of iterations	28,596	43,780	69,882	144,095	185,939	387,218	514,644	816,158	853,110	606,128
VVM	Convergence	Yes	Yes	Yes	Yes	Yes	No	Yes	Yes	No	No
	ε_1 (percent)	47.340	52.006	53.966	61.092	61.826	–	62.983	60.348	–	–
	Number of iterations	28,508	43,220	68,694	142,138	183,482	–	529,294	783,426	–	–

Note: [a]Convergent to unreasonable results

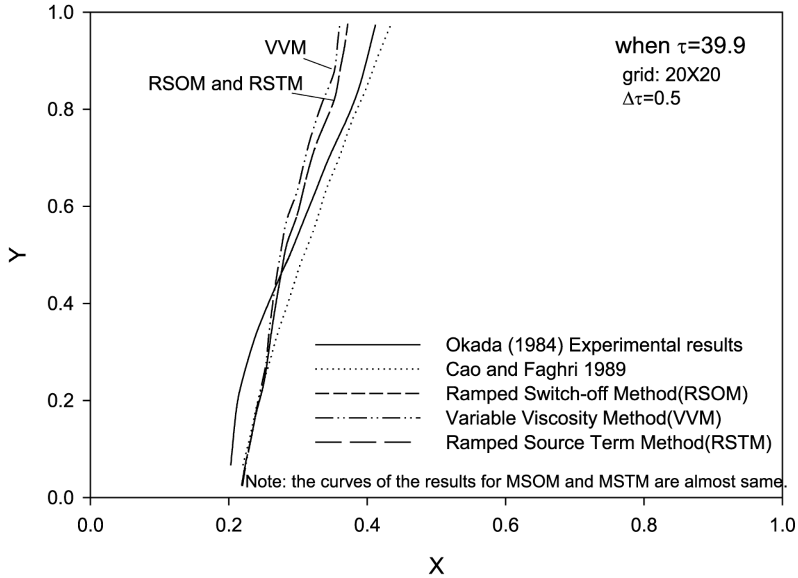

Figure 2. Comparison of the locations of the melting fronts at $\tau = 39.9$ (grid size: 20×20, time step $\Delta\tau = 0.5$)

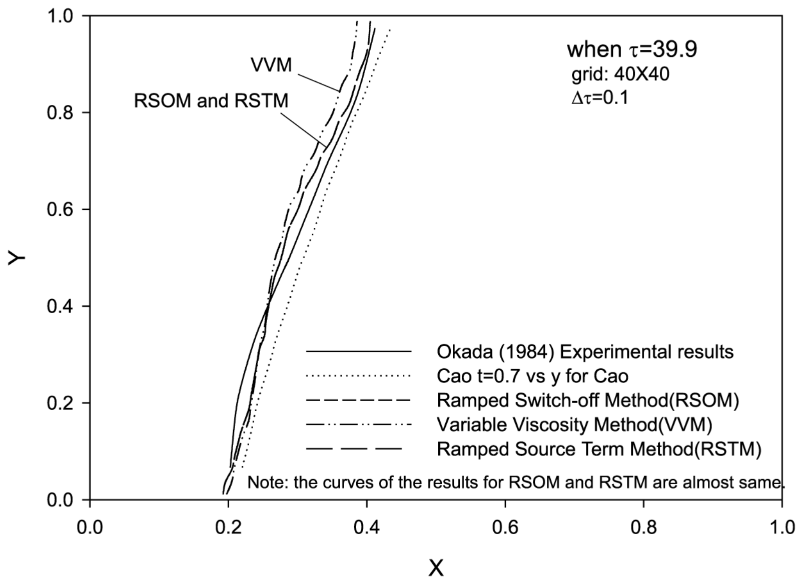

Figure 3. Comparison of the locations of the melting fronts at $\tau = 39.9$ (grid size: 40×40, time step $\Delta\tau = 0.1$)

Comparison between VVM and RSOM/RSTM. The ε_l in the tables and the positions of melting fronts shown in the figures indicate that the numerical results obtained by VVM is slightly smaller than that obtained by RSOM and RSTM. On the other hand, the number of iterations required for simulation based on VVM is a little bit less than the number of iterations required for simulation based on RSOM or RSTM. In the

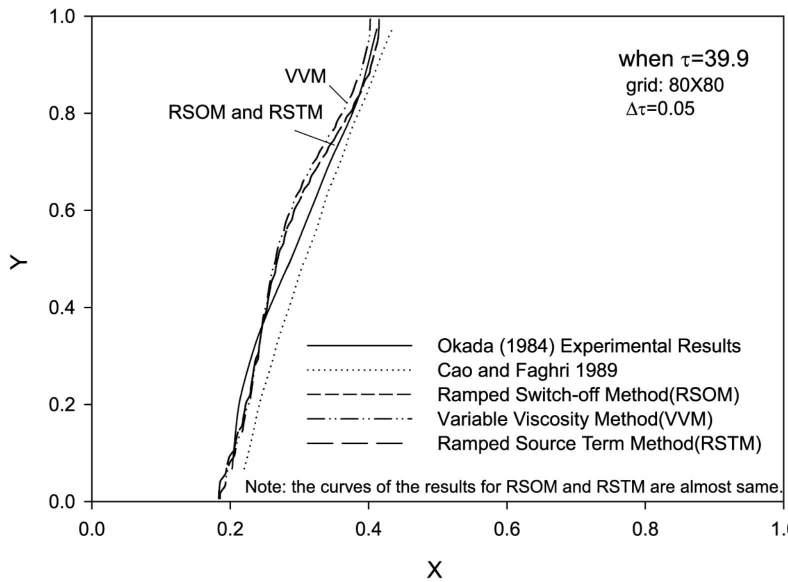

Figure 4.
Comparison of the locations of the melting fronts at $\tau = 39.9$ (grid size: 80×80, time step $\Delta\tau = 0.05$)

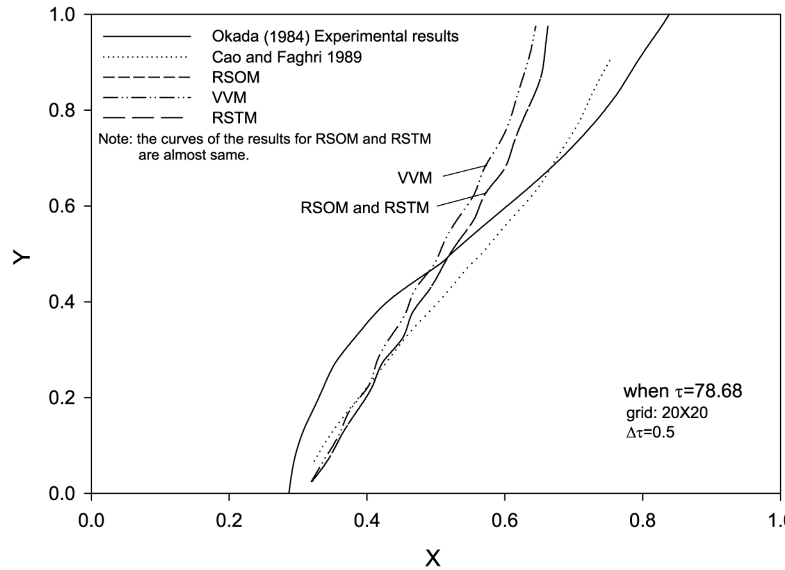

Figure 5.
Comparison of the locations of the melting fronts at $\tau = 78.68$ (grid size: 20×20, time step $\Delta\tau = 0.5$)

figures the position of the melting fronts obtained by RSOM/RSTM are much closer to the experimental results (Okada, 1984) than those results obtained by VVM. Thus we conclude that the RSOM and RSTM scheme is more accurate than VVM and, therefore, should be chosen as the solid velocity correction scheme for research in phase-change problems if TTM is applied. Note that non-ramped SOM and STM described in Section

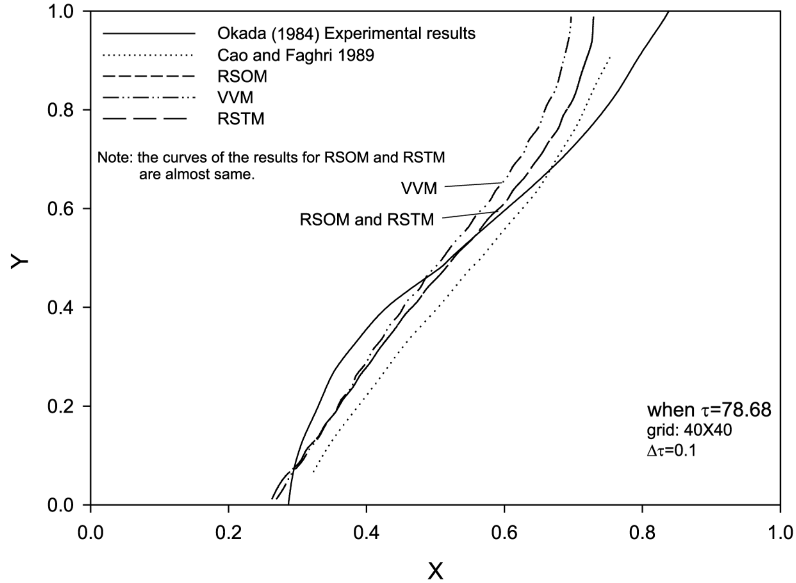

Figure 6.
Comparison of the locations of the melting fronts at $\tau = 78.68$ (grid size: 40×40, time step $\Delta\tau = 0.1$)

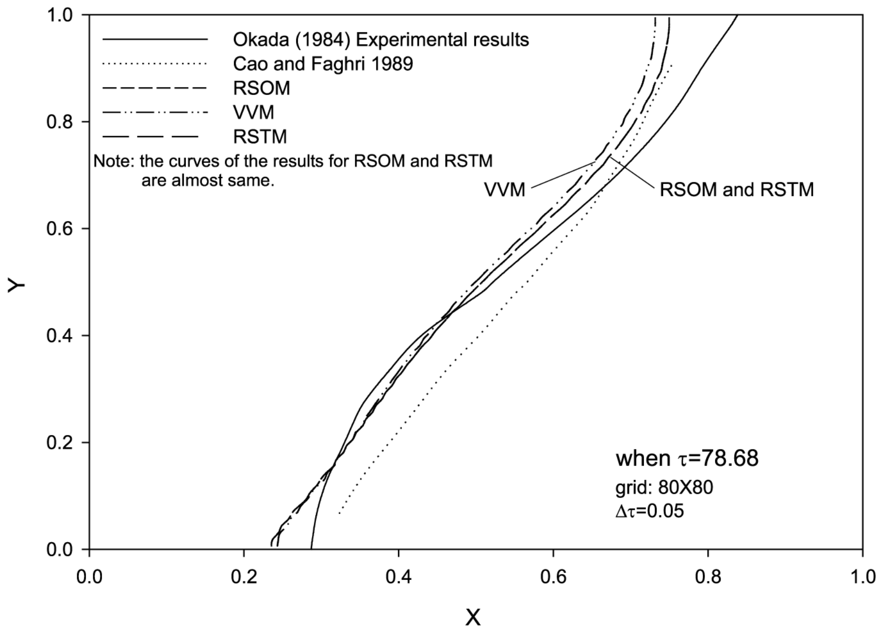

Figure 7.
Comparison of the locations of the melting fronts at $\tau = 78.68$ (grid size: 80×80 time step $\Delta\tau = 0.05$)

3.2, however, are not acceptable in TTM simulations for convection controlled phase-change problems as we have discussed in Section 3.2.

Consistency of discretized TTM. Model inconsistency exists in all three of these schemes. In Tables IV-VI, it is clear that when the time step is too small compared with the grid size, the simulation results will either blow up to infinity or converge to an unreasonable result, while with a comparatively large time step the simulation results are acceptable. In Figures 8 and 9 RSOM is used as example and we find that when time step is too small compared with the grid size (in Figure 8, $\Delta\tau = 0.001$ with grid size 40×40; in Figure 9, $\Delta\tau = 0.01$ with grid size 20×20) the positions of the melting

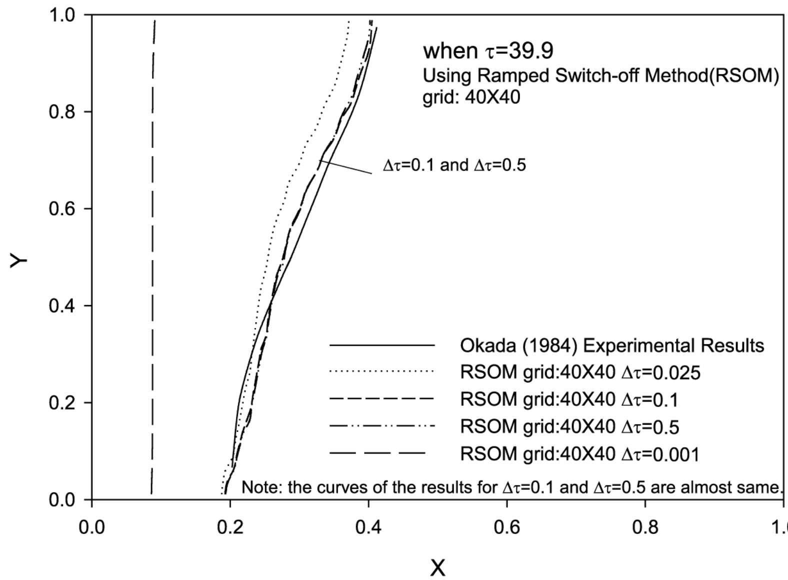

Figure 8.
Comparison of the locations of the melting fronts at $\tau = 39.9$ (RSOM, grid size: 40×40)

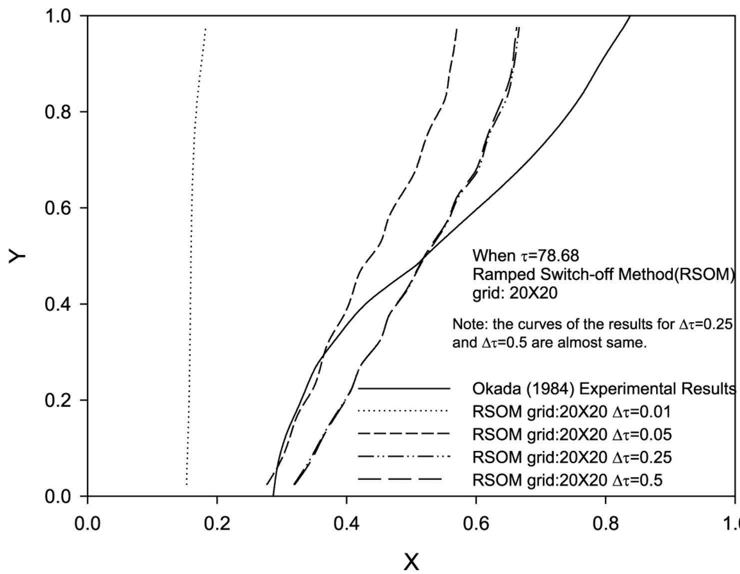

Figure 9.
Comparison of the locations of the melting fronts at $\tau = 78.68$ (RSOM, grid size: 20×20, time step varies)

fronts are much closer to the left boundary than they should be, and those fronts are nearly perpendicular to x-axis. From those results, as well as unreasonably almost zero velocity profiles U and V we see in the liquid region (located between the left boundary and the melting front) during simulations in those cases, we conclude that once $\Delta\tau/\Delta X\Delta Y$ is smaller than around $60 \sim 80$, an area playing a role as "transient zone", the discretized TTM model obtained by the finite volume method tends to be incapable of describing the convection effect during a heat transfer process. Even if the simulation results exist, they are more and more similar to those from pure-conduction cases when $\Delta\tau/\Delta X\Delta Y$ goes to zero. (See the tendency of simulation results of RSOM/RSTM in Tables IV-VI when $\Delta\tau/\Delta X\Delta Y < 60$). This is a typical manifestation of "inconsistency". This is because when $\Delta\tau/\Delta X\Delta Y$ goes to zero, the system of algebraic equations is no longer equivalent to the original partial differential equations at each grid point (See Fletcher, 1991 for a complete definition of consistency). In RSOM and RSTM the inconsistency causes the model to become a pure-conduction case when $\Delta\tau/\Delta X\Delta Y$ is too small. On the other hand, in VVM, the inconsistency is expressed by the simulation results blowing up (Tables IV-VI). Therefore, to avoid divergence or convergence to an unreasonable result, the time step must be chosen carefully so that it is not too small and it matches the grid size. For instance, keeping $\Delta\tau/\Delta X\Delta Y$ larger than 80 in the current simulation will guarantee convergent results (Tables IV-VI). The inconsistency of the discretized TTM model is an interesting phenomenon and needs thorough theoretical analysis to obtain more insight.

Note that clearly a too large value of $\Delta\tau/\Delta X\Delta Y$ will cause coarse results due to large time steps. The results showed in Tables IV-VI and Figures 8-11 indicate that the accuracy will be best when $\Delta\tau/\Delta X\Delta Y$ is chosen between $10^2 \sim 10^3$.

Cost-effective concerns. From Tables IV-VI we find as grid numbers increase, the chance of divergence decrease although the number of total iterations significantly increases. Larger grid numbers only slightly change the simulation results. On the

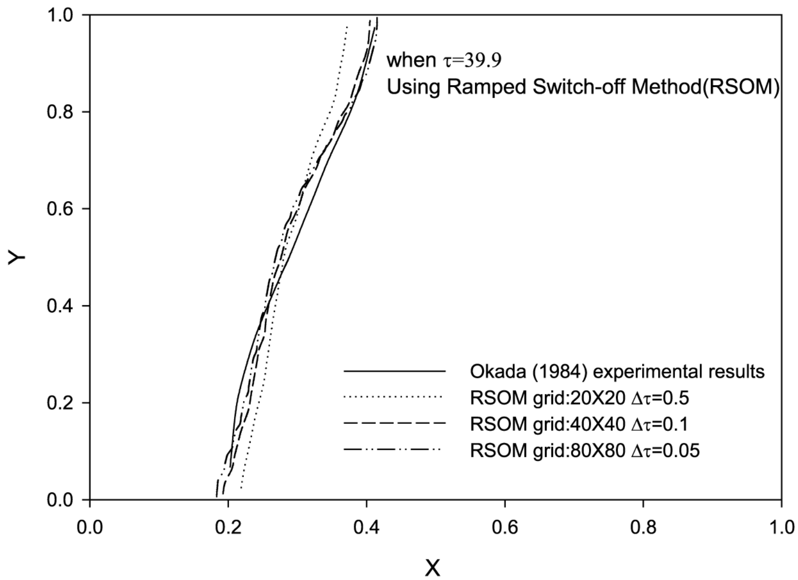

Figure 10.
Comparison of the locations of the melting fronts at $\tau = 39.9$ (RSOM with different grid sizes and time steps)

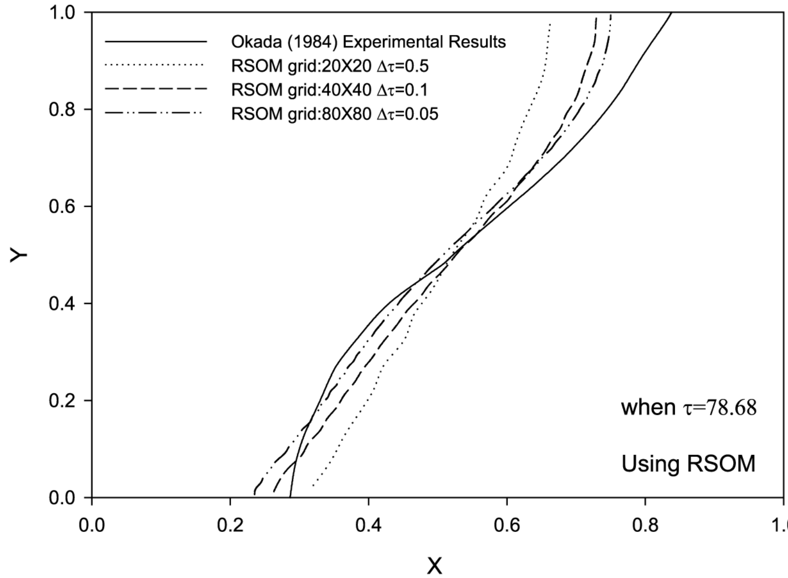

Figure 11.
Comparison of the locations of the melting fronts at $\tau = 78.68$ (RSOM with different grid sizes and time steps)

other hand, we also find that with a fixed grid number the difference among the results obtained by using different time-steps from 1 to 0.01 (if the results converged reasonably) is not significant although the running time increases considerably when using a small time-step. More important and convincible results are shown in Figures 10 and 11 where the results of different combinations of grid sizes and time steps are compared. We find that although the results of grids: 20×20, $\Delta\tau = 0.5$ case is not good, both the results of the 40×40, $\Delta\tau = 0.1$ case and 80×80, $\Delta\tau = 0.05$ case are acceptably accurate. However, since the simulation time of the 80×80, $\Delta\tau = 0.05$ case is remarkably longer than that of the 40×40, $\Delta\tau = 0.1$, if the cost is a concern it is better to choose the time-step length around 0.1 and the grid number of around 40×40.

An additional numerical test was done based also on experimental results in Okada (1984) in order to validate the above finding. All parameters and set up are the same as in the former example except that in this case (referred to “Okada, 1984 case 2”) $Ra = 6.95 \times 10^5$, $Ste = 0.0959$. Results are listed in Table VII, Figures 12 and 13, where we see the results match our conclusion made above, i.e. in the zone where the numerical model is consistent, RSOM and RSTM generate almost identical results; VVM runs with less iterations but also less accuracy; the choice of RSOM/RSTM with grid size 40×40, $\Delta\tau = 0.1$ is the best one balancing the cost and efficiency.

Table VII.
Simulation results of Okada (1984) case 2 (stopped when $\tau = 30$)

	RSOM grid 20×20 $\Delta\tau = 0.5$	RSOM grid 40×40 $\Delta\tau = 0.1$	RSOM grid 80×80 $\Delta\tau = 0.05$	RSTM grid 40×40 $\Delta\tau = 0.1$	VVM grid 40×40 $\Delta\tau = 0.1$
ε_l (percent)	47.561	50.565	49.777	50.565	48.812
Number of iterations	33,428	97,206	224,293	97,197	92,979

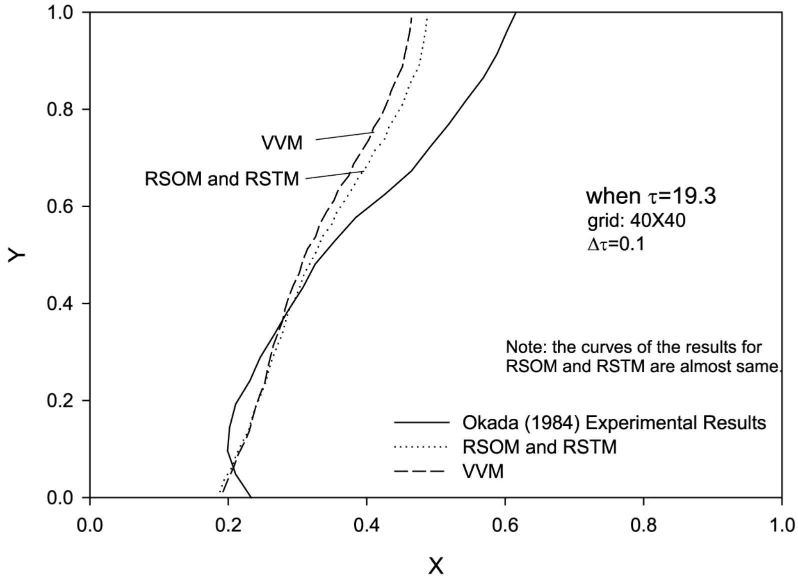

Figure 12.
Comparison of the locations of the melting fronts at $\tau = 19.3$ (grid size: 40×40, time step $\Delta\tau = 0.1$)

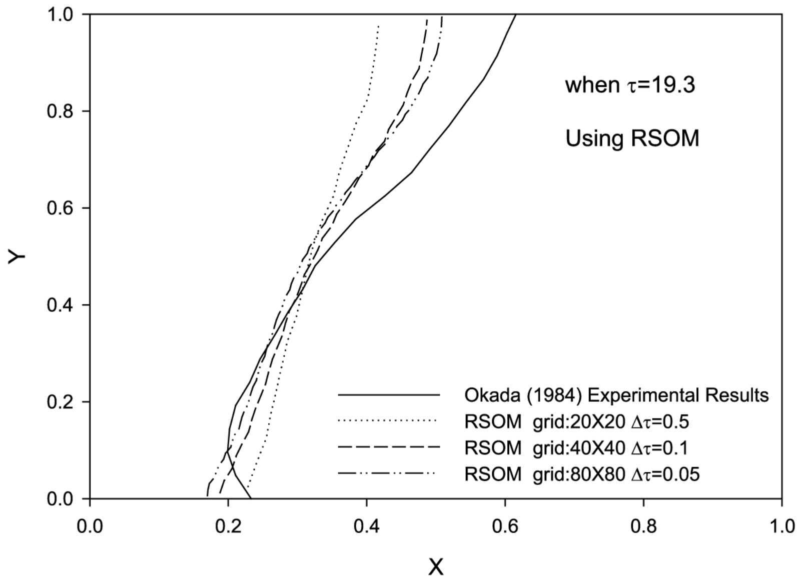

Figure 13.
Comparison of the locations of the melting fronts at $\tau = 19.3$ (RSOM with different grid sizes and time steps)

5. Conclusions

Effects of solid velocity correction schemes on a TTM for convection controlled solid-liquid phase-change problem are investigated in this paper. While the TTM is a simple and accurate enough model for simulation and analysis of convection/diffusion phase-change problems, the inconsistency of this model is exposed during our variable grid sizes/time step simulation tests. We conclude that in order to efficiently use the discretized TTM model and obtain convergent and reasonable results, we must choose a grid size with a suitable time step (which should not be too small). We discussed the commonly used solid velocity correction schemes, SOM, STM and VVM, and then validated ramped SOM (RSOM) and STM (RSTM) procedures in which we introduce a "linear" mushy region to improve the simulation performance of the original SOM and STM. The simulation results using RSOM, RSTM and VVM in TTM are compared with experimental results, and from this we conclude that combined with TTM, RSOM and RSTM present almost identical results which are more accurate than VVM. As Voller *et al.* (1987) pointed out, though the ramped velocity correction schemes have physical importance only for phase changes with existence of mushy regions, mathematically they can also be used for isothermal phase-change simulations as a choice of numerical discretization.

References

Binet, B. and Lacroix, M. (2000), "Melting from heat sources flush mounted on a conducting vertical wall", *Int. J. Num. Meth. Heat & Fluid Flow*, Vol. 10, pp. 286-306.

Brent, A.D., Voller, V.R. and Reid, K.J. (1988), "Enthalpy-porosity technique for modeling convection-diffusion phase change: application to the melting of a pure metal", *Numerical Heat Transfer*, Vol. 13, pp. 297-318.

Cao, Y. and Faghri, A. (1990), "A numerical analysis of phase change problem including natural convection", *J. Heat Transfer*, Vol. 112, pp. 812-15.

Fletcher, C.A.J. (1991), *Computational Techniques for Fluid Dynamics: Fundamental and General Techniques*, Springer, New York, NY.

Gartling, D.K. (1980), "Finite element analysis of convective heat transfer problems with change of phase", in Morgan, K., Taylor, C. and Brebbia, C.A. (Eds), *Computer Methods in Fluids*, Pentech, London, pp. 257-84.

Hsiao, J.S. (1984), "An efficient algorithm for finite difference analysis of heat transfer with melting and solidification", *ASME* Paper No. WA/HT-42.

Morgan, K. (1981), "A numerical analysis of freezing and melting with convection", *Comp. Meth. App. Eng.*, Vol. 28, pp. 275-84.

Mundra, K., DebRoy, T. and Kelkar, K.M. (1996), "Numerical prediction of fluid flow and heat transfer in welding with moving heat source", *Numerical Heat Transfer, Part A*, Vol. 29, pp. 115-29.

Okada, M. (1984), "Analysis of heat transfer during melting from a vertical wall", *Int. J. Heat Mass Transfer*, Vol. 27, pp. 2057-66.

Pantankar, S.V. (1980), *Numerical Heat Transfer and Fluid Flow*, McGraw-Hill, New York, NY.

Sasaguchi, K., Ishihara, A. and Zhang, H. (1996), "Numerical study on utilization of melting of phase change material for cooling of a heated surface at a constant rate", *Numerical Heat Transfer, Part A*, Vol. 29, pp. 19-31.

Viskanta, R. (1983), "Phase change heat transfer", in Lane, G.A. (Ed.), *Solar Heat Storage: Latent Heat Materials*, CRC Press, Boca Raton, FL, pp. 153-222.

Voller, V.R. (1997), "An overview of numerical methods for solving phase change problems", in Minkowycz, W.J. and Sparrow, E.M. (Eds), *Advances in Numerical Heat Transfer*, Vol. 1, Taylor & Francis, Basingstoke.

Voller, V.R., Cross, M. and Markatos, N.C. (1987), "An enthalpy method for convection/diffusion phase change", *Int. J. Num. Meth. Eng.*, Vol. 24, pp. 271-84.

Yang, M. and Tao, W.Q. (1992), "Numerical study of natural convection heat transfer in a cylindrical envelope with internal concentric slotted hollow cylinder", *Numerical Heat Transfer, Part A*, Vol. 22, pp. 289-305.

Yao, L.C. and Prusa, J. (1989), "Melting and freezing", *Advances in Heat Transfer*, Vol. 25, pp. 1-96.

Zhang, Y. and Faghri, A. (1996), "Heat transfer enhancement in latent heat thermal energy storage system by using an external radial finned tube", *J. Enhanced Heat Transfer*, Vol. 3, pp. 119-27.

Zhang, Y. and Faghri, A. (1999), "Vaporization, melting and heat conduction in the laser drilling process", *Int. J. Heat Mass Transfer*, Vol. 42, pp. 1775-90.

Zhang, Y., Faghri, A., Buckley, C.W. and Bergman, T.L. (2000), "Three-dimensional sintering of two-component metal powders with stationary and moving laser beams", *ASME Journal of Heat Transfer*, Vol. 122, pp. 150-8.

Corresponding author
Yuwen Zhang is the corresponding author and can be contacted at: zhangyu@missouri.edu